

Optical conductivity of Ortho-II $\text{YBa}_2\text{Cu}_3\text{O}_{6.5}$

E. Bascones¹, T. M. Rice¹, A.O. Shorikov², V.I. Anisimov²

¹*Theoretische Physik, ETH-Hönggerberg, CH-8050 Zurich (Switzerland)*

²*Institute of Metal Physics, 620219 Ekaterinburg, GSP-170 (Russia)*

(Dated: February 2, 2008)

The Ortho-II phase of $\text{YBa}_2\text{Cu}_3\text{O}_{6.5}$ is characterized by a periodic alternation of empty Cu and filled Cu-O b-axis chains doubling the unit cell in the a direction. The extra oxygen in the full chains gives rise to an attractive potential for the holes in the planes. The planar bands split in two with a gap opening at the new Brillouin zone boundary $k_x = \pm\pi/2$, which we estimate from LDA calculations. Using a planar model which treats the d-wave superconductivity in a mean field approximation, we show that interband transitions produce a strongly anisotropic feature in the optical conductivity controlled by a region in \vec{k} -space close to $(\pi/2, \pi/2)$. The edge position of this feature gives information on the temperature dependence of quasiparticle spectrum in this region. Bilayer splitting would show up as a double edge shape.

PACS numbers: 74.72-h, 74.25, 78.30.-J, 71.27+a

Highly ordered Ortho-II $\text{YBa}_2\text{Cu}_3\text{O}_{6.5}$, with an average doping per planar Cu $x \sim 0.1$ and a $T_c \sim 60$ K, is a suitable system to study the properties of underdoped cuprates and the effect of the chains on the superconducting planes in YBCO. The Ortho-II phase is characterized by a periodic alternation of filled and empty Cu-O b-axis chains, doubling the size of the unit cell in the a direction¹. The oxygen ordering reduces the disorder and highly ordered samples have been prepared². Unfortunately YBCO is not suitable for the angle-resolved photoemission (ARPES) measurements³ due to poor quality of the cleaved surface, but it is a convenient system for infrared experiments.

In this letter we analyze how the oxygen ordering affects the band structure and optical conductivity of Ortho-II $\text{YBa}_2\text{Cu}_3\text{O}_{6.5}$. The presence of oxygen in the chains gives rise to an attractive potential for the holes in the planes. Due to the alternation of empty and filled chains, this potential is $2a$ periodic. This causes a reduction of the Brillouin zone in the Gx direction (see notation in Fig. 1) with the corresponding splitting of the bands. We find a highly anisotropic optical conductivity due to interband transitions between the split bands, characterized by a sharp-edge peak in the a direction, while it vanishes at threshold in the b direction. These features should be absent in non-Ortho II phases. The conductivity onset of absorption is controlled by a region in \vec{k} -space close to $(\pi/2, \pi/2)$ and the position of the threshold depends on the quasiparticle dispersion in this region and on the value of the interband gap.

The normal state of underdoped cuprates has an anisotropic gap, with an overall d-wave dependence. ARPES measurements suggest⁴ that with decreasing temperature, the opening of the gap removes larger portions of the Fermi surface (FS) resulting in Fermi arcs close to the nodal direction. The size of these arcs shrink to a point upon entering the superconducting state. In a bilayer material interplanar coherence appears as a splitting of the planar bands, and consequently of the FS branches, into bonding (B) and antibonding (A) states

$\epsilon_{A,B}(\mathbf{k}) = \epsilon_{pl}(\mathbf{k}) \pm t_{\perp}(\mathbf{k})$. The existence of bilayer splitting (BS) in the antinodal region in the overdoped regime is widely accepted^{5,6}. On the contrary, results in the nodal direction^{7,8}, as well as in the underdoped and optimally doped regimes^{7,9,10,11,12,13,14} remain controversial. We show that the dependence of the Ortho-II interband transition threshold on the gap amplitude allows one to extract information on these questions from infrared measurements.

We have performed LDA¹⁵ calculations using the TB-LMTO-ASA computation scheme¹⁶. $\text{YBa}_2\text{Cu}_3\text{O}_{6.5}$ crystallizes in orthorhombic structure (space group Pmmm). The following lattice parameters obtained at room temperature¹⁷ $a=7.659\text{\AA}$ $b=3.872\text{\AA}$ and $c=11.725\text{\AA}$ were used in calculations. The basis of muffin-tin orbitals contained $(3s, 2p, 3d)$ orbitals for O, $(4s, 4p, 3d)$ orbitals for Cu, $(5s, 5p, 4d, 4f)$ orbitals for Y and $(6s, 6p, 5d, 4f)$ orbitals for Ba atom. A k -point mesh of $6 \times 4 \times 2$ was used for self consistency calculation loop. As suggested by recent NMR experiments¹⁸, the $2a$ periodicity arising from the Ortho-II ordering produces a charge imbalance between the Cu atoms below a filled and an empty chain. Evidence of charge modulation on the order of 0.05 in planar Cu has been found in resonant soft X-ray scattering rate¹⁹. We have calculated the charge distribution in the Cu atoms using the same size for all Cu spheres. Our estimation for the charge modulation in Cu ions (including the occupation of all the orbitals in the basis) is on the order of 0.06 holes in the planes.

The calculated band structure is shown in Fig. 1. The band marked with dots is the single chain band which crosses the Fermi level, associated with the filled chain. Rough estimate of the volume enclosed by the Fermi surface of the chain bands leads to 0.04 ± 0.01 holes per Cu in the planes. This value is smaller than expected, what could be due to deviations of LDA predictions close to the insulating phase. The effect of the $2a$ periodicity is reflected in the band structure. The planar B and A states each split in two bands. The splitting of the bands shows up clearly in the XS and RU directions, at which

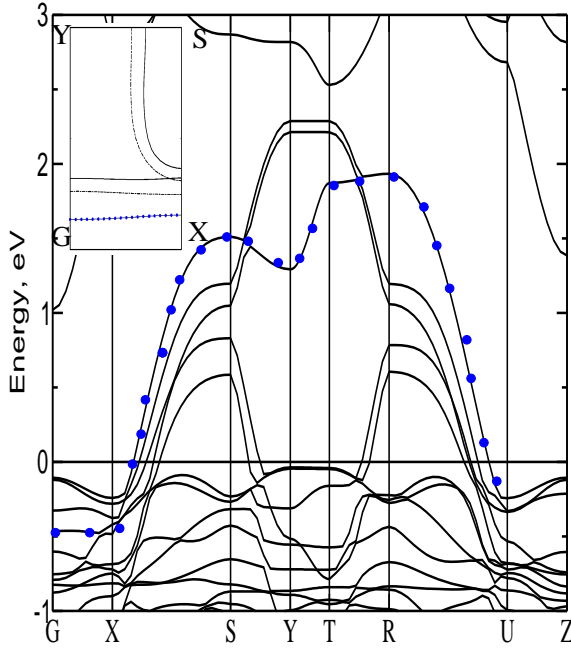


FIG. 1: Main figure: Band structure obtained from LDA calculations. The band marked with dots is chain-like. $G = (0, 0, 0)$, $X = (\pi/2, 0, 0)$, $S = (\pi/2, \pi, 0)$, $Y = (0, \pi, 0)$, $T = (0, \pi, \pi)$, $R = (\pi/2, \pi, \pi)$, $U = (\pi, 0, \pi)$, $Z = (0, 0, \pi)$. Inset: LDA Fermi surface in the G-X-S-Y plane. The chain branch is enhanced with dots. Solid (dot-dashed) lines correspond to the split B (A) bands.

the Brillouin zone has folded. The four planar bands appear in two pairs. Intra and inter-pair splitting are due to interlayer coherence and oxygen ordering respectively. Without the doubling of the unit cell both band pairs would be degenerate. The interband transitions discussed below connect lower (α) and upper (β) band states with the same bilayer symmetry. LDA calculations show a k -dependent $\alpha(\beta)$ splitting. On the Fermi level, in the XS direction, it varies between 120 and 160 meV independent of the bilayer band. The FS is shown as an inset. The chain branch is enhanced with dots. B and A branches are in solid and dashed-dot lines respectively. β bands have quasi-onedimensional character. This quasi-onedimensionality has been used to explain the anisotropy of the elastic scattering rate of Ortho-II $YBa_2Cu_3O_{6.5}$ ²⁰. B and A bands cut the XS line at $B\alpha$, $B\beta$ and $A\alpha$, $A\beta$ respectively. Note that BS does not vanish at the nodes in LDA.

To calculate the optical conductivity we use a planar

dispersion

$$\epsilon(\mathbf{k}) = -2t(\cos k_x + \cos k_y) + 4t' \cos k_x \cos k_y - 2t''(\cos 2k_x + \cos 2k_y) - \mu \quad (1)$$

$k_x, k_y \in (-\pi, \pi)$ in lattice parameter units, which we take equal for a and b axes. The alternation of empty and filled chains is introduced by an external potential $V \sum_{i,j,P=1,2,\sigma} c_{2i,j,\sigma}^{P\dagger} c_{2i,j,\sigma}^P$ where i, j label sites in a and b direction, P the two superconducting planes. The interlayer hopping is $t_{\perp}(\mathbf{k})$. In the reduced Brillouin zone $k_x \in (-\pi/2, \pi/2)$, $k_y \in (-\pi, \pi)$ the resulting dispersion is

$$\epsilon_{\alpha,\beta}^L(\mathbf{k}) = -2t \cos k_y - 2t''(\cos 2k_x + \cos 2k_y) - \mu \pm t_{\perp}(\mathbf{k}) \pm \left(4 \cos^2 k_x (t - 2t' \cos k_y)^2 + \frac{V^2}{4} \right)^{1/2} \quad (2)$$

First plus and minus signs correspond to $L = A$ and B and second signs to α and β , respectively. Since in LDA calculations V and $t_{\perp}(\mathbf{k})$ are only slightly \vec{k} -dependent near the nodes, we set them constant.

To describe the d-wave superconducting state we introduce a phenomenological attractive potential of the form $V_0(\cos k_x - \cos k_y)(\cos k'_x - \cos k'_y)$ which reflects the symmetry of the underlying Cu-O plaquette. Thermal²¹ and microwave conductivity²² measurements performed in Ortho-II $YBa_2Cu_3O_{6.5}$ have found that its superconducting quasiparticles are well defined BCS excitations corresponding to an anisotropic low-energy gap with nodal lines. In the following, superconductivity is treated at the mean field level in the new split bands. Only intraband and interband pair scattering processes $(\gamma, \mathbf{k}, \sigma; \gamma, -\mathbf{k}, \sigma) \rightarrow (\gamma', \mathbf{k}', \sigma'; \gamma', -\mathbf{k}', -\sigma')$, with $\gamma, \gamma' = \alpha, \beta$ are kept. The presence of the $2a$ periodic potential breaks the rotation symmetry of the d-wave gap and, in the reduced Brillouin zone, it takes the form: $\Delta_{\alpha,\beta}(\mathbf{k}) = \frac{1}{2}\Delta_0(g(\mathbf{k}) \cos k_x - \cos k_y)$ with

$$g(\mathbf{k}) = \frac{2 \cos k_x (t - 2t' \cos k_y)}{\left(4 \cos^2 k_x (t - 2t' \cos k_y)^2 + \frac{V^2}{4} \right)^{1/2}} \quad (3)$$

The breaking of the tetragonal symmetry shifts slightly the position of the nodes, with a maximum shift at $k_x = 0$. Here we take $\Delta_0 = 71$ meV for both B and A bands^{5,12,21}.

In linear response the real part of the optical conductivity reads

$$\sigma^{ii}(\omega) = \frac{2e^2}{\nu\omega} \sum_{\mathbf{k},L} M^{ii}(\mathbf{k}) \left[\frac{1}{2} \left(1 - \frac{\epsilon_{\alpha}^L(\mathbf{k})\epsilon_{\beta}^L(\mathbf{k}) + \Delta_{\alpha}(\mathbf{k})\Delta_{\beta}(\mathbf{k})}{E_{\alpha}^L(\mathbf{k})E_{\beta}^L(\mathbf{k})} \right) [1 - n_F(E_{\alpha}^L(\mathbf{k})) - n_F(E_{\beta}^L(\mathbf{k}))] \delta(\omega - (E_{\alpha}^L(\mathbf{k}) + E_{\beta}^L(\mathbf{k}))) \right. \\ \left. + \frac{1}{2} \left(1 + \frac{\epsilon_{\alpha}^L(\mathbf{k})\epsilon_{\beta}^L(\mathbf{k}) + \Delta_{\alpha}(\mathbf{k})\Delta_{\beta}(\mathbf{k})}{E_{\alpha}^L(\mathbf{k})E_{\beta}^L(\mathbf{k})} \right) [n_F(E_{\alpha}^L(\mathbf{k})) - n_F(E_{\beta}^L(\mathbf{k}))] \delta(\omega - |E_{\beta}^L(\mathbf{k}) - E_{\alpha}^L(\mathbf{k})|) \right] \quad (4)$$

Here, ν and e are the volume of the sample and the electronic charge, $E_{\alpha,\beta}^L = \sqrt{\epsilon_{\alpha,\beta}^{L2}(\mathbf{k}) + \Delta_{\alpha,\beta}^2(\mathbf{k})}$ are the quasiparticle energies in the superconducting state, n_F is the Fermi distribution function and $M^{ii}(\mathbf{k})$ the matrix elements in the a and b directions.

$$M^{aa}(\mathbf{k}) = \frac{V^2(t - 2t' \cos k_y)^2 \sin^2 k_x}{4 \cos^2 k_x(t - 2t' \cos k_y)^2 + \frac{V^2}{4}} \quad (5)$$

$$M^{bb}(\mathbf{k}) = \frac{4V^2 t'^2 \sin^2 k_y \cos^2 k_x}{4 \cos^2 k_x(t - 2t' \cos k_y)^2 + \frac{V^2}{4}} \quad (6)$$

The terms in parenthesis in (4) are the well known coherence factors. When $\Delta_{\alpha}(\mathbf{k}) = \Delta_{\beta}(\mathbf{k}) = 0$ the first (second) factor vanishes if the states involved in the transition are on the same (different) side of the FS. The first term in (4) accounts for the contribution of those transitions which produce an excitation in both the α and β bands. The second term includes transitions which transfer a thermal excitation from one band to another.

Upper part of Fig. 2 show the optical conductivity in the a and b directions for parameters which mimic reasonably well the LDA bands and FS in the GXSY plane. We take $t = 360$ meV, $t'/t = 0.3$, $t''/t = 0.15$, $V = 120$ meV $\mu = -243$ meV and $t_{\perp} = 135$ meV. Fig. 2a) show the a-axis conductivity in the superconducting (main figure) and normal, gapless, case (inset) at zero temperature. In the normal state the conductivity is characterized by a sharp single peak with an onset energy $\omega = 120$ meV, while in the superconducting state it shows a double peak. At $T = 0$ there are no excitations in the system and the second term in (4) vanishes. Only those transitions which cross E_F are allowed. The minimum energy for the transition, and consequently the onset for absorption, is $\omega = V = 120$ meV²³ and corresponds to the states with $k_x = \pm\pi/2$ between the two branches of the same bilayer FS, i.e. states between $A\alpha$ and $A\beta$, and between $B\alpha$ and $B\beta$ (and the corresponding ones in the other quadrants) in the inset of Fig. 1. Note the vicinity of these points to the nodal direction. Only these states contribute to the conductivity at threshold.

A finite superconducting gap increases the energy of the transitions. The minimum energy still corresponds to a state at the edge of the zone, between the two normal state FS branches. The double peak lineshape in the superconducting state marks the threshold energy for transitions in the B (lower onset) and A (higher onset) bands. The onset of interband transitions in the B-band

occurs for \vec{k} -points close to the nodes in the superconducting gap while in its A-band the relevant region of \vec{k} -space is further away from the nodes, leading to a double peak structure. The experimental observation of a double edge would be a clear evidence of the existence of BS in the underdoped regime.

The peak lineshape is due to the \vec{k} dependence of the matrix element $M^{aa}(\mathbf{k})$. $M^{aa}(\mathbf{k})$ is finite and large at $k_x = \pm\pi/2$, and decreases away from the zone boundary, thus the conductivity decreases with increasing ω . In the normal state, the peak in the conductivity is enhanced by an approximate one-dimensional behavior of the transition energy for \vec{k} between the two FS branches close to $k_x = \pi/2$. This is also the reason of the larger magnitude of the first peak in the conductivity in the superconducting state. This strong enhancement would be smoothed by a k_y dependent splitting at the XS direction, as the one shown in Fig. 1, and, therefore, could be absent experimentally.

Opposite to the behavior in the a-direction, $M^{bb}(\mathbf{k})$ vanishes at $k_x = \pm\pi/2$, resulting in a vanishing $\sigma^{bb}(\omega)$ at the threshold frequency, as shown in Fig. 2b) for the normal (inset) and superconducting state. In the superconducting state the BS splitting would appear in the b-axis conductivity as a double hump. The difference in intensity in the a- and b- directions is striking. The anisotropy in intensity and lineshape can be used experimentally to identify the interband transition.

Correlation effects renormalize the band structure with respect to the LDA predictions. In the lower part of Fig. 2 we plot the optical conductivity in the a direction, at zero (Fig. 2c) and finite (Fig. 2d) temperature, for the case in which the Fermi velocity has been reduced to the half of its previous value. The bilayer splitting has been adjusted such that the doping in the bonding (antibonding) band is 0.05 holes below (above) the average doping¹¹. Correlations are not expected to affect the Hartree potential due to the oxygen ordering, and we keep it unchanged. The qualitative features in the conductivity remain. Quantitatively the peak splitting has been slightly reduced and the bonding threshold deviates a bit from the gapless value.

Fig. 2d shows the optical conductivity in the a direction σ^{aa} at $T = 60$ K. At finite temperatures the existence of excitations reduce the contribution of the first term in (4) decreasing the amplitude of the zero temperature peak. The second term in (4) starts to contribute, and, in the presence of a gap, is responsible of a small structure

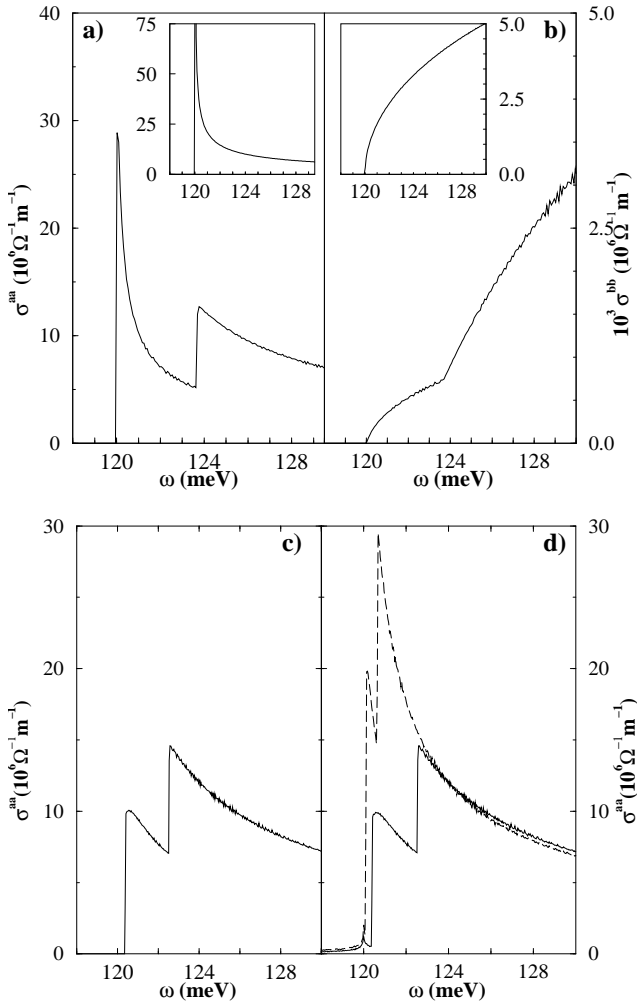


FIG. 2: Figs. a) and b) Optical conductivity in the a and b directions, respectively, in the normal gapless case (insets) and in the superconducting state (main figures) for the parameters given in the text that mimic the LDA calculations. Note the different scale in the axis of a) and b). The axis and units of each inset are equal to the ones in the corresponding figure. Figures c) and d) show the optical conductivity in the a direction in the superconducting state for the renormalized dispersion: $t = 180 \text{ meV}$, $\mu = -156 \text{ meV}$ and $t_{\perp} = 26 \text{ meV}$, t'/t , t''/t and V are kept as a), see text. The values of μ and t_{\perp} correspond to a doping $x_A = 0.15$ and $x_B = 0.05$ holes in the A and B bands, respectively. c) shows the zero temperature conductivity for $\Delta_0 = 71 \text{ meV}$. In d) the conductivity at 60 K corresponding to $\Delta_0 = 71 \text{ meV}$ (solid line) and to $\Delta_0 = 35.5 \text{ meV}$ (dashed line) is plotted.

which appears at $\omega \sim V$ and below. However, at the temperatures of interest $T \sim T_c$ these effects are very small. On the other hand, if the superconducting gaps in the region of \vec{k} -space controlling these peaks are reduced with increasing temperature, the onsets for conduction and the peak splitting also decrease. This can be clearly seen in Fig. 2d, where the a-axis conductivities for two different values of Δ_0 are compared. The evolution of the position of the peaks with increasing temperature gives us information on the modification of the superconducting gap in the region of \vec{k} -space where the FS cuts the XS direction.

In the pseudogap state, upon crossing T_c superconducting coherence is lost, but a gap remains in the antinodal spectrum. To describe the loss of coherence in (4) we set $\Delta_{\alpha}(\mathbf{k})\Delta_{\beta}(\mathbf{k}) = 0$ in the coherence factors, but keep the same value (with gap) in the excitation energies $E_{\alpha}^L(\mathbf{k})$ and $E_{\beta}^L(\mathbf{k})$. This is equivalent to the condition, in the Nambu-Gorkov formalism, that the anomalous Green functions vanish. The energy of the interband transition does not change. Since in the superconducting state, the values of $\Delta_{\alpha}(\mathbf{k})$ and $\Delta_{\beta}(\mathbf{k})$ are small in the area of \vec{k} -space which controls the conductivity close to threshold, this modification has little effect on the lineshape, and the discussion above remains valid even if superconducting coherence is lost.

In summary we predict an anisotropic feature in the infrared optical conductivity of Ortho-II $YBa_2Cu_3O_{6.5}$, which should be absent in non Ortho-II phases. It is a consequence of the oxygen ordering in every second chain. Possible bilayer splitting would cause a double edge shape. The threshold energy and its evolution with temperature give information on the quasiparticle spectrum close to the nodes and on the effect of the chains on the planar electronic structure. Preliminary experimental results²⁴ have not shown any signature clearly identifiable with the one predicted here. The estimated intensity of this feature is comparable with the Drude contribution. Its appearance is based on the existence of quasiparticles. This picture seems to be well justified in the superconducting state at low temperatures and low energies^{21,22}. Its absence, if confirmed, could point out to a breakdown of the quasiparticle description at higher energies.

Financial support from Swiss National Science Foundation and NCCR MANEP and from grants RFBR-0402-16096, RFBR-03-02-39024 and URO-SO-22 is gratefully acknowledged.

¹ N.H. Andersen *et al*, Physica C **317-318**, 259 (1999).

² R. Liang, D.A. Bonn, W. N. Hardy, Physica C **336**, 57 (2000).

³ A. Damascelli, Z. Hussain and Z.-X. Shen, Rev. Mod. Phys. **75**, 473 (2003).

⁴ M.R. Norman *et al*, Nature (London) **392**, 157 (1998).

⁵ D.L. Feng *et al*, Phys. Rev. Lett. **86**, 5550 (2001).

⁶ Y.-D. Chuang *et al*, Phys. Rev. Lett. **87**, 117002 (2001).

⁷ A.A. Kordyuk *et al*, cond-mat/0311137.

⁸ O.K. Andersen, A.I. Liechtenstein, O. Jepsen and F.

Paulsen, J. Phys. Chem Solids, **56**, 1573 (1995).

⁹ A. Kaminski *et al*, Phys. Rev. Lett. **90**, 207003 (2003).

¹⁰ Y.-D. Chuang *et al*, cond-mat/0107002.

¹¹ A.A. Kordyuk *et al*, Phys. Rev. B **66**, 014502 (2002).

¹² S.V. Borisenko *et al*, Phys. Rev. B **66**, 140509 (R) (2002).

¹³ S.V. Borisenko *et al*, Phys. Rev. Lett. **90**, 207001 (2003).

¹⁴ S.V. Borisenko *et al*, cond-mat/0312036.

¹⁵ W. Kohn, Rev. Mod. Phys. **71**, 1253 (1999)

¹⁶ O.K. Andersen *et al*, Rev. Rev. Lett. **53**, 2571 (1984)

¹⁷ J. Grybos *et al*, Physica C **220**, 138-142 (1994)

¹⁸ Z. Yamani *et al*, cond-mat/0310255

¹⁹ D.L. Feng *et al*, cond-mat/0402488

²⁰ R.G. Harris, Phd Thesis. The University of British Columbia, October 2003.

²¹ M. Sutherland *et al*, Phys. Rev. B **67**, 174520 (2003).

²² P.J. Turner *et al*, Phys. Rev. Lett. **90**, 237005 (2003).

²³ The conductivity includes the contribution of transitions in both the bonding and antibonding states, which, as suggested by the LDA calculations have the same onset. If the periodic potential seen by the bonding and antibonding bands were different, each band would have a different optical threshold and the conductivity would show more structure, with two peaks and a double hump in the a and b directions, respectively.

²⁴ T. Timusk, private communication.